On the Scaling of the Critical Solution Temperature of Binary Polymer Blends with Chain Length

Fernando A. Escobedo[†,‡] and Juan J. de Pablo[*,†]

Department of Chemical Engineering, University of Wisconsin, Madison, Wisconsin 53706-1691, and School of Chemical Engineering, Cornell University, Ithaca, New York 14853-5201

Received August 4, 1998; Revised Manuscript Received November 25, 1998

ABSTRACT: Monte Carlo simulations have been performed to examine the scaling with chain length of the upper critical solution temperature (T_c) of binary, symmetric blends of polymers. Critical parameters were obtained by histogram reweighting analysis of semigrand canonical ensemble simulations near the critical temperature. For several continuum space polymeric models, it is found that $T_c/\tilde{\epsilon}$ scales approximately as either $\rho_c(A + B\,N)$ or $\rho_c N/(B^{-1} + A/\sqrt{N})$, where N is chain length, ρ_c is the density at T_c, $\tilde{\epsilon}$ is a chemical mismatch parameter, and A and B are constants that depend on the specific characteristics of the model. Constant A provides a measure of the correction to the Flory−Huggins' prediction $T_c \sim N$. The effect of such correction term becomes unimportant for large N, $\tilde{\epsilon}$, and temperature. Excellent agreement is found, however, with the mean-field prediction that $\chi^E \sim 2/N$ (for all systems studied), where χ^E is a continuum space, enthalpic "chi" parameter which takes into account the variations of local structure of the fluid for different chain lengths at the critical point.

I. Introduction

Blending of polymers provides a convenient means to prepare materials with properties intermediate to those of the components. Unfortunately, it is difficult to achieve miscibility in nonpolar polymers; typically, the presence of a small chemical mismatch suffices to cause phase separation. This effect can be conveniently explained in the framework of the Flory−Huggins theory.[1] In this theory, the expression for the free energy of mixing per total number of monomers is

$$\beta\Delta F_{mix} = \frac{\phi_1}{N_1}\ln\phi_1 + \frac{\phi_2}{N_2}\ln\phi_2 + \chi\phi_1\phi_2 \qquad (1)$$

where N_i and ϕ_i are the chain length and monomer fraction of species i, respectively, and χ is the interaction parameter:

$$\chi = \frac{z_{ef}}{k_B T}\left(\epsilon_{12} - \frac{1}{2}\epsilon_{11} - \frac{1}{2}\epsilon_{22}\right) = \beta z_{ef}\,\bar{\epsilon} \qquad (2)$$

In eq 2, z_{ef} is an effective coordination number, k_B is Boltzmann constant, T is temperature, $\beta = (k_B T)^{-1}$, and ϵ_{ij} is the energy of interaction between two neighbor sites of types i and j (e.g., $i, j = 1$ or 2).

In eq 1, the first two terms on the right-hand side represent the ideal, combinatorial entropy of mixing, and the last term represents the enthalpy of mixing. This theory predicts that for high polymers (N_1 and $N_2 \to \infty$) ΔF_{mix} will be dominated by the enthalpic term. As the temperature is raised, $\chi \to 0$ and any positive enthalpy of mixing will eventually become small enough to allow the polymers to mix; consequently, the phase diagram for such systems will exhibit an upper critical solution temperature (to be denoted as T_c).

In eq 1 it is assumed that deviations from ideal mixing arise only from energetic effects. Such an assumption is incorrect; it has been shown by theory and simulation[2−4] that even systems with $\chi = 0$ can phase separate if the components differ sufficiently in backbone flexibility.[3,4] This behavior is caused by differences in structural properties between components (e.g. packing of molecules) which also contribute to the excess free energy of mixing.

For a symmetric blend ($N_1 = N_2 = N$), the critical point is determined by evaluating $\partial^2\beta\Delta F/\partial\phi_1^2 = 0$ and $\partial^3\beta\Delta F/\partial\phi_1^3 = 0$ in eq 1; this yields $\phi_1 = \phi_2 = \phi_c = 0.5$ and

$$\chi_c = 2/N \qquad (3)$$

Sanchez and Lacombe[5,6] developed a "lattice-fluid" theory that incorporates vacancies in the lattice, thereby allowing for density fluctuations in the system (e.g., compressibility effects). It can be shown that for a symmetric blend at the critical point, the Sanchez−Lacombe theory (and other compressible Flory−Huggins type theories) leads to $\phi_c = 0.5$ and

$$\chi_c = 2/(N\bar{\rho}) \qquad (4)$$

where $\bar{\rho}$ is a dimensionless density, reduced with respect to the closed-packed density of the system. Equation 4 reduces to Flory's result (eq 3) when no vacancies are allowed, e.g., if $\bar{\rho} = 1.0$ (alternatively, $\bar{\rho}$ could be introduced in the definition of χ). Equation 4 underlines the importance, often overlooked, of density on χ_c. It should be noted that the renormalization of χ by density is also predicted by other theories; for instance, the polymer reference interaction site model (PRISM)[7] leads to a definition for χ' that incorporates a proper density factor.

In experimental work, effective χ^{SANS} parameters are often extracted from the static structure factor [measured by small angle neutron scattering (SANS) experiments] by adopting the random phase approximation expression of deGennes.[8] The χ parameters extracted from this approach can typically be described by the

[†] University of Wisconsin.
[‡] Cornell University.

10.1021/ma9812276 CCC: $18.00
Published on Web 01/20/1999

empirical form[11]

$$\chi^{\mathrm{SANS}} = \frac{a_1}{T} + a_0 \tag{5}$$

where a_0 and a_1 are adjustable constants, which in general depend on composition and density. At the critical point, from eqs 2, 3, and 5 we get

$$\frac{1}{k_B T_c} = \frac{b_1}{N} + b_0 \tag{6}$$

Other investigators[12,18] have used instead an empirical linear model to correlate T_c with chain length:

$$k_B T_c \approx c_0 + c_1 N \tag{7}$$

In eqs 6 and 7, the b and c are system specific constants. Constant b_0 (or c_0) is thought to arise from energetic and entropic effects (e.g. chain-end effects, shape asymmetries, etc.). In general, models depicted in eqs 6 and 7 behave differently in the asymptotic limits of N small and N large. Other semitheoretical models have been proposed to describe the scaling of T_c with chain length. For example, Holyst and Vilgis[9] employed field-theoretical methods to obtain self-consistent expressions for the critical value of χ, which incorporate ideal chain conformation and fluctuation corrections to the Flory–Huggins theory; for a symmetric binary blend the result is[10]

$$\chi_c = \frac{2}{N}[1 + a'/\overline{N}] \tag{8}$$

where a' is an adjustable parameter. Equation 8 is not consistent with either eq 6 or eq 7. Although in the limit of $N \to \infty$ the simple Flory–Huggins $T_c \sim N$ scaling is recovered from eqs 7 and 8, significant departures from this behavior can be expected in blends comprising low-to-intermediate molecular weight polymers (which are ubiquitous in commercial polydisperse systems). It is the purpose of this work to study in more detail how T_c in polymer blends approaches the linear scaling regime.

Symmetric polymer blends represent one of the chemically simplest systems that exhibit an upper critical solution temperature; they have been the subject of much theoretical work,[7,12,13,15,16] molecular simulation studies,[17–19,21,22] and experimental work.[23] Most of these studies have concurred that $T_c \sim N$ and that the constant b_0 (in eq 6) or c_0 (in eq 7), if existent, is a small number. PRISM theory[12,13] (with molecular closures) and simulation results for incompressible systems[17–19,21] indicate that the linear scaling $T_c \sim N$ is established for fairly short chains (e.g. $N \sim 10$). These studies and the experimental work of Gehlsen and co-workers[23] with isotopic blends are considered by many to have settled any questions regarding the validity of the linear scaling of T_c with N (at least for high polymers such as those employed by Gehlsen et al.).

Important questions remain, however, regarding the onset of the scaling regime and the role of density, small mixture asymmetries, etc. For example, the experimental study of Gehlsen et al.[23] is only concerned with the scaling of χ_c (not T_c) with N; a wide range of densities was not investigated. Results from incompressible PRISM[12] indicate that the predicted scaling law is sensitive to the closure relation employed and, when a linear scaling is attained, the magnitude and sign of c_0 (eq 7) also depend on the closure equation employed. A compressible PRISM formalism presented by Gromov and de Pablo[22] predicts that, at constant-pressure conditions and for low to intermediate molecular weight chains, $T_c \sim N^\gamma$ with γ being system dependent (which takes on the questionable value of $\gamma \sim 0.55$ for the particular model studied by these authors). The lattice cluster theory[14,15] and a compressible version of Flory–Huggins theory[16] (similar to that of Sanchez and Lacombe[5]) have also been employed to examine the scaling of T_c and the Ginzburg number (Gi) with chain length for symmetric and asymmetric polymer blends. For a specific, nearly symmetric blend at constant pressure, the lattice cluster theory predicts that T_c varies linearly with N (e.g., eq 7).[15] While the incompressible Flory–Huggins theory predicts that both T_c/N and $Gi \times N$ are constant, the compressible version leads to nonconstant values for these quantities.[16] Since the Ginzburg number roughly delineates the temperature range where either mean-field or Ising-type behavior applies, a nonconstant $Gi \times N$ could have a important effect on the scaling of all critical properties. Further, the incompressible Flory–Huggins theory fails to predict that, at T_c and normal pressure, the density of high molecular weight polymer blends will become too low to be consistent with liquid melts.[16]

It is also important to point out that simulation results have been, with the exception of two recent studies,[21,22] concerned exclusively with lattice systems. It has been noted that packing effects in a bond fluctuation model (which has been adopted for many studies of blend phase behavior) are less pronounced than in continuum space models;[25] consequently, local correlations in the polymeric fluid may not be accurately described in such lattice studies. The importance of structural correlations is evident when a continuum space definition of χ is examined. Since z_{ef} in eq 2 can be interpreted as the number of monomers that lie (on average) within the first solvation layer surrounding a given site, following Grest et al.[21] we write[38]

$$\chi^{E} = \frac{z_{ef}\bar{\epsilon}}{k_B T} \tag{9}$$

$$z_{ef}\,\bar{\epsilon} = \rho \int_0^\infty \left[U_{12}(r) - \frac{1}{2}U_{11}(r) - \frac{1}{2}U_{22}(r)\right] g_{12}(r)\, \mathrm{d}\mathbf{r} \tag{10}$$

where $U_{ij}(r)$ is the energy of interaction between sites i and j located at a distance r apart, and $g_{12}(r)$ is the probability of finding sites of types 1 and 2 (from different molecules) at a distance r apart. In the Flory–Huggins theory $z_{ef}\bar{\epsilon}$ is a constant; in general, however, it will depend on temperature, chain length, composition, and density. At constant density, one would expect that at high enough temperatures (e.g. long chains or repulsive systems), $g_{12}(r)$ becomes independent of T or N (the long-chain athermal limit). At constant pressure, however, density changes will also have some effect on $g_{12}(r)$. Because T_c is coupled to N, the overall effect of chain length on $g_{12}(r)$ could be lumped into the so-called *correlation hole effect*. Müller and Binder[26] found that for athermal lattice polymers, the effective coordination number (of hypothetical thermal interactions) for chains of length N, $z_{ef}(N)$, follows the relation

$$z_{ef}(N) = z_{ef}(\infty) + \frac{\mathrm{const}}{N^{1/2}}$$

Such a variation of z_{ef} is due to the correlation hole effect (whose correlation length is commensurate to the chain radius of gyration $N^{1/2}$) and must affect the scaling of χ_c with N. These effects are different from those due to the crossover from Ising to mean-field behavior previously described in connection with the theory of Holyst and Vilgis (eq 8). In their study of asymmetric polymer mixtures (and retrospective calculations for symmetric mixtures) on a lattice, Müller and Binder[26] found that while eq 7 provides a good correlation to simulation data, the relative deviation of simulated T_c from the mean-field predicted value vanishes approximately as $1/N^{1/2}$; it is unclear, however, how such deviations are related to both critical fluctuations and correlation hole effects.

In this study, we reexamine the scaling of T_c and χ_c with N based on simulation of continuum-space polymeric systems for longer chain lengths and more realistic molecular interactions than those employed in the aforementioned simulation studies. In addition, we study the effect of the details of the interaction potentials, thermal expansion, and density fluctuations (through constant pressure simulations) on the scaling behavior of T_c and χ.

II. Models and Methodology

In this work, a polymer chain is modeled as a collection of freely jointed interaction sites; bonded sites are held together by rigid links of length l. All blends are symmetric, i.e., they are composed of two homopolymers (species 1 and 2) of length N which are structurally identical. Two molecular models are adopted, an "attractive" system in which sites experience a modified Lennard−Jones type of interaction energy, and a "repulsive" system in which sites are essentially hard spheres with an added repulsive energy for unlike-species interactions. Our modified cut-and-shifted Lennard−Jones (MLJ) potential energy function between sites i and j is defined as

$$\begin{aligned} u_{ij}(r) &= \infty, \quad r < \lambda_{ov}\sigma \\ &= F_{ij}(r) - F_{ij}(\lambda_{cut}\sigma), \quad \lambda_{ov}\sigma \le r \le \lambda_{cut}\sigma \\ &= 0, \quad r > \lambda_{cut}\sigma \end{aligned} \tag{11}$$

where

$$F_{ij}(x) = -4\epsilon_{ij}\left[\left(\frac{\sigma}{x}\right)^{12} - \left(\frac{\sigma}{x}\right)^{6}\right]$$

and we set $\lambda_{ov} = 0.96$ and $\lambda_{cut} = 1.57$; these values were selected based on purely computational grounds, as they increase significantly the efficiency of molecular rearrangement moves and volume fluctuations for large polymeric systems. The bond length was fixed at $l = \lambda_{ov}\sigma$. The same values of σ and λ are used for like- and unlike-species interactions, but $\epsilon_{12} = \epsilon_{21} > \epsilon_{11} = \epsilon_{22} = \epsilon$. A chemical mismatch parameter is defined as

$$\tilde{\epsilon} = \frac{1}{\epsilon_{11}}\left[\epsilon_{12} - \frac{1}{2}(\epsilon_{11} + \epsilon_{22})\right] = \frac{\epsilon_{12}}{\epsilon} - 1 \tag{12}$$

Site−site interactions in the repulsive mixtures are described by the same function of eq 11 but now

$$F_{ij}(x) = -\epsilon_{ij}\left[\left(\frac{\sigma}{x}\right)^{6}\right]$$

and $\lambda_{ov} = 1$, $\lambda_{cut} = 1.6$, $l = \sigma$, $\epsilon_{11} = \epsilon_{22} = 0$, and $\epsilon_{12} = 1$. In this case, there is no attractive energy between sites and we simply define $\tilde{\epsilon} = \epsilon_{12}$. Like monomers experience a hard-core repulsion, while unlike monomers experience a hard-core excluded volume interaction plus a soft, short-ranged repulsion.

All simulations were conducted in the framework of a semigrand ensemble, in which the total number of chains in the system $M = M_1 + M_2$, the temperature, and the difference in chemical potential between species $\Delta\mu = \mu_1 - \mu_2$ are all fixed during the course of a calculation. Composition fluctuations are introduced by moves that change the identity of a chain from one species to the other.[17] A convenient order parameter to measure composition changes is

$$\tilde{M} = M_1 - M_2$$

An attempt to change the identity of a randomly chosen molecule is accepted with the probability

$$P_{acc} = \min\left(1, \exp\left[-\beta\Delta U + \beta\frac{\Delta\tilde{M}}{2}\Delta\mu\right]\right) \tag{13}$$

where ΔU and $\Delta\tilde{M}$ represent the change in energy and order parameter, respectively, between the proposed and the current configurations of the system. As previously shown in lattice[17−20] and continuum space simulations,[3,21] these identity-change moves are the key to effective sampling of composition fluctuations in polymeric systems. Note, however, that they are only directly applicable to species of similar architecture. For a symmetric mixture, $\Delta\mu = 0$.

Simulations can be conducted at constant volume (and therefore density) or at constant pressure. Rearrangements of polymeric sites were performed by a combination of extended continuum configurational-bias moves,[27] reptation, translation, and rotation moves.[31] Moves that exchange the identity between two chains of different species were also employed; these moves change the spatial distribution of molecules of a given species but do not change the composition of the system. Volume changes required for constant-pressure simulations were performed by conventional rescaling of molecular centers of mass.

Histograms of energy, order parameter, and volume (if not constant) were recorded during the simulations. These histograms were then combined to estimate the ensemble probability distribution within a range of temperatures by employing a multihistogram reweighting technique MHR,[28] which permits extrapolation of properties measured at one set of conditions (of, e.g., temperature) to other neighboring conditions. Details on the application of this method can be found elsewhere.[19] At temperatures below T_c, the histogram of $\tilde{M}$ at coexistence conditions becomes bimodal with two symmetric peaks; if these peaks have little overlap, they can be used with confidence to estimate the binodal composition of each coexistence phase. As the UCST is approached, however, the two peaks overlap significantly and finite size effects become more pronounced (the correlation length of composition fluctuations can exceed the size of the simulation box); when this occurs, it is difficult to extract reliable coexistence compositions. Fortunately, the position of the critical point can be estimated from such simulations by employing a finite-size scaling analysis.[19,20,29]

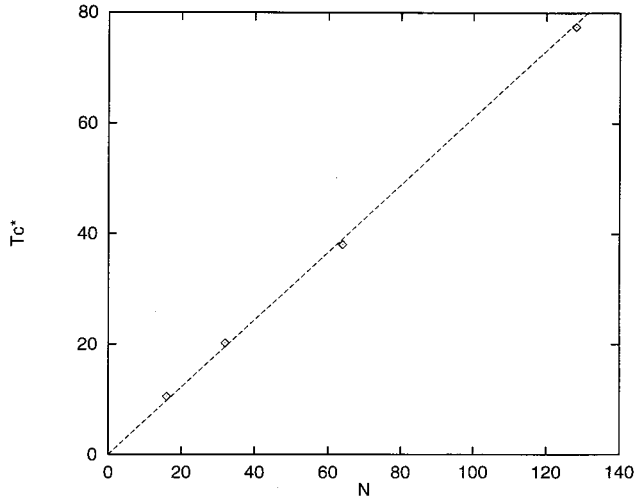

Figure 1. Critical temperatures as a function of chain length for the repulsive systems. Simulation data are shown by symbols; the line is a fit of the form $T_c = 0.61 \times N$.

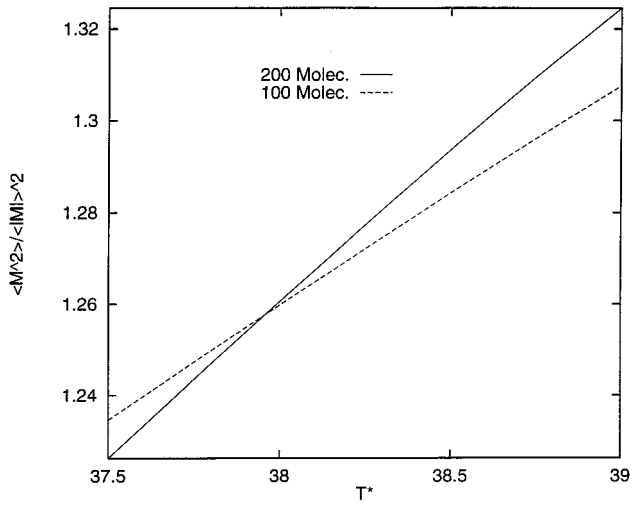

Figure 2. Data for the crossing of the ratio of moments $\langle M^2\rangle/\langle|M|\rangle^2$ for repulsive blend of 64-mers. The moments are calculated for two different system sizes, namely, 120 and 60 molecules.

The system sizes employed in this work ranged from $M = 250$ molecules for $N = 32$ to $M = 90$ for $N = 380$. Systems with about half these sizes were employed for the finite-size scaling estimation of critical temperatures. The critical temperature was estimated by the crossing of the ratio of suitable moments of $\tilde{M}$, $R_M = \langle\tilde{M}^2\rangle/\langle|\tilde{M}|\rangle^2$, computed for two system sizes (as described in detail by Deutsch and Binder[18,19]). The required moments of the order parameter $\tilde{M}$ were obtained from the multihistogram method for a range of temperatures in the vicinity of T_c.

III. Results

A. Constant Density Systems. Simulations at constant density have the advantage that they can cover a wide range of temperatures while avoiding vaporization of the polymer. Note, however, that the pressure of a given system will increase as the temperature is raised. Also, the system effectively becomes a mixture of supercritical fluids above the vapor−liquid critical temperature of the polymer.

Simulation results for repulsive blends (system V-0) were conducted at a constant site-number density of $\rho^* = \rho\sigma^3 = 0.7$; the calculated critical temperatures ($T_c^* = k_B T_c/\epsilon_{12}$) are presented in Figure 1 and in Table 1. Figure 2 shows typical data for the crossing of the dimensionless ratios of moments to determine the location of the critical temperature. Figure 3 shows the peculiar shape of the histograms for these systems. From Figure 1 it is evident that $T_c \sim N$, even for the range of short chain-lengths covered by these simulations. This observation agrees with that reported by Grest et al.,[21] who simulated an off-lattice symmetric mixture of chains with purely repulsive interactions. In their simulations, Grest at al. employed soft-core sites (the repulsive part of a 6:12 potential); an energy parameter $\tilde{\epsilon}$ (defined as in eq 12) was varied at constant temperature to induce phase separation. Changes in $\tilde{\epsilon}$ are reminiscent of changes in deuterium concentration in isotopic mixtures.[23] The advantage of our hard-core model is that changes in our energy parameter $\tilde{\epsilon}$ (from eq 12) have a one-to-one correspondence with changes in temperature; consequently, no ambiguity exists in establishing the scaling of T_c with chain length (this equivalence is only approximate in the model of Grest et al.).

Table 1. Critical and χ Parameters for the MLJ and Repulsive Systems

system	chain length	T_c^*	ρ_c^*	χ^{MF}, eq 2	χ^{E}, eq 9
V-0	16	10.5(3)	0.7	2.55	2.09
($\rho^* = 0.70$, $\tilde{\epsilon} = 1$)	32	20.2(6)	0.7	2.65	2.07
	64	38.0(9)	0.7	2.82	2.07
	128	77.5(9)	0.7	2.77	2.06
V-1	64	0.805(3)	0.825	2.31	2.10
($\rho^* = 0.825$, $\tilde{\epsilon} = 0.01$)	128	1.49(3)	0.825	2.50	2.04
	256	2.73(4)	0.825	2.73	2.02
	380	3.85(5)	0.825	2.87	2.05
V-2	128	0.682(4)	0.90	2.08	2.10
($\rho^* = 0.900$, $\tilde{\epsilon} = 0.0035$)	256	1.16(6)	0.90	2.45	2.12
	380	1.67(8)	0.90	2.53	2.08
V-3	32	0.926(4)	0.70	2.56	2.03
($\rho^* = 0.700$, $\tilde{\epsilon} = 0.03$)	64	1.647(6)	0.70	2.87	2.03
	128	3.06(5)	0.70	3.10	2.06
	256	5.93(6)	0.70	3.17	2.04
P-1	32	0.532(4)	0.897(5)	1.90	2.08
($P^* = 0.0$, $\tilde{\epsilon} = 0.01$)	64	0.758(5)	0.772(5)	2.30	2.07
	128	0.974(9)	0.598(7)	2.77	1.94
P-2	64	0.422(6)	0.958(5)	1.79	2.10
($P^* = 0.0$, $\tilde{\epsilon} = 0.0035$)	128	0.622(8)	0.866(6)	2.20	2.12
	256	0.855(8)	0.720(6)	2.67	2.07
	380	0.994(10)	0.590(6)	2.78	1.97

Three types of MLJ systems were considered for the constant-volume simulations to be denoted V-1, V-2, and V-3, for which we adopted [$\tilde{\epsilon} = 0.01$, $\rho^* = 0.9$], [$\tilde{\epsilon} = 0.0035$, $\rho^* = 0.825$], and [$\tilde{\epsilon} = 0.03$, $\rho^* = 0.7$], respectively. Constant density simulations of the MLJ systems must contend with the fact that, for a given density, there is a lower limit of chain length below which the system becomes "glassy" (see also discussion in the next section). Figure 4 shows renormalized critical temperatures ($T_c^*/\rho_c^*\tilde{\epsilon}$, where $T^* = k_B T_c/\epsilon_{11}$) as a function of chain length; numerical data are summarized in Table 1. Note that the vapor-liquid critical temperature of the pure monomer system is $T^* = 0.57$.[36] The trends shown in Figure 4 are approximately linear with nonzero intercept. However, results for longer chain lengths are necessary to unambiguously establish the linear character of these trends.

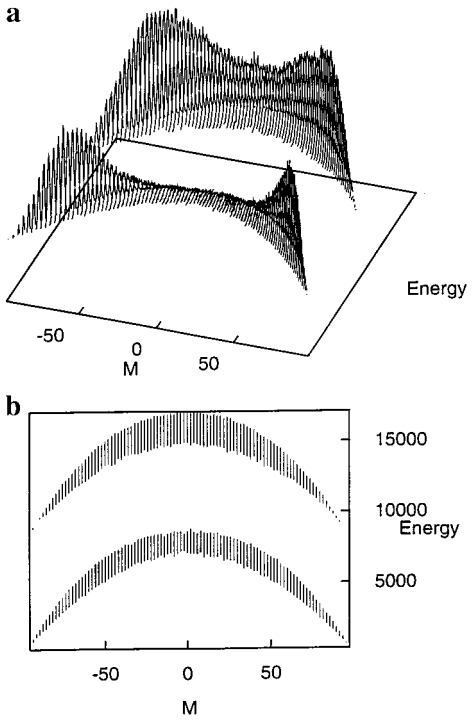

Figure 3. Shape of the histograms for the repulsive blend of 64-mers. The histograms at the bottom of the figures correspond to $T^* = 35$, and those at the top of the figure are for $T^* = 38.75$ (the estimated critical point of the system is 38.0). To facilitate the comparison, the energy scale for the histograms at $T^* = 38.75$ have been shifted up by 8000 units.

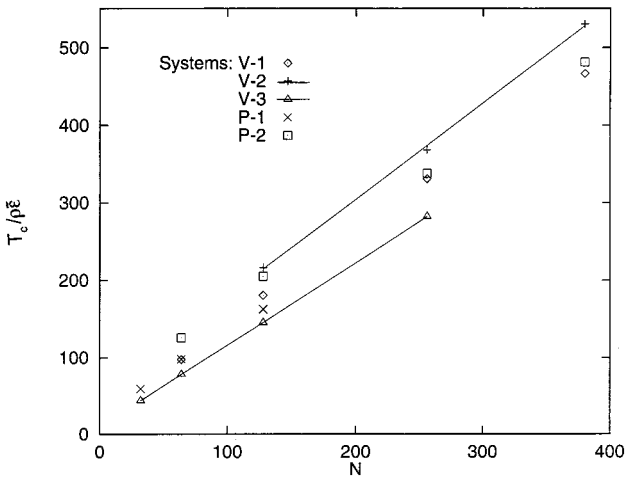

Figure 4. Renormalized critical temperatures $T_c/(\rho^*\tilde{\epsilon})$ as a function of chain length for blends at constant density (V-1, V-2, and V-3), and blends at constant zero pressure (P-1 and P-2). The chemical mismatch parameter $\tilde{\epsilon}$ is set to 0.01 for systems V-1 and P-1, $\tilde{\epsilon} = 0.0035$ for systems P-1 and P-2, and $\tilde{\epsilon} = 0.03$ for system V-3. The lines are just guides to the eye.

In order to apply the Flory−Huggins theory to our constant-density systems, vacancies are included (at a volume fraction = ϕ_V = constant); the binodal curve is given by

$$T^* = \frac{N z_{ef}(1-\phi_V)\,\tilde{\epsilon}\,(1-2\phi_i)}{\log(1/\phi_i - 1)}, \quad 0 < \phi_i < 0.5 \quad (14)$$

where $\tilde{\phi}_i = \phi_i(1-\phi_V)$ (ϕ_i is the volume fraction of species i). Figure 5 compares the predictions of eq 14 for our V-3 system (dashed lines) to simulation data (full lines); for this application, we chose the value of $z_{ef}(1-\phi_V)$ in

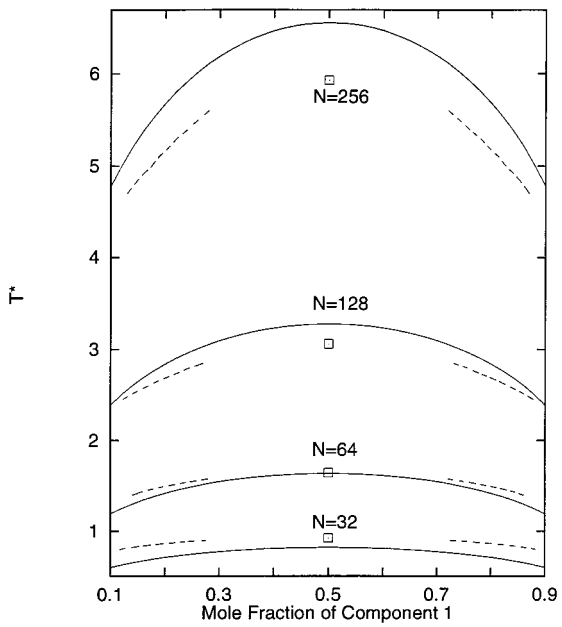

Figure 5. Simulated (full lines) and theoretical (dashed lines) binodal curves for system V-3 (see Table 1). Simulated critical points are shown by squares. Theoretical predictions are based on Flory−Huggins theory fitted to the critical point for the $N = 64$ system. Simulated binodal curves are shown here by curves (and not by symbols) because individual simulated points can be smoothly connected by employing histogram reweighting; near the critical point, however, finite-size scaling is required to obtain reliable binodal compositions (which was only done to extract critical points).

eq 14 to match the simulated critical temperature for the $N = 64$ system. This type of fitting procedure is not uncommon in experimental work. It is seen in Figure 5 that the shape of the binodal curves is not correctly predicted by Flory−Huggins theory and that T_c is underestimated for $N < 64$ and overestimated for $N > 64$. If eq 14 (with the same fitted constant) is used for the V-1 and V-2 systems, the changes in the binodal curves (caused by the different $\tilde{\epsilon}$ and ϕ_V) are qualitatively captured, but deviations from simulation data are even greater than those shown in Figure 5.

B. Constant Pressure Systems. Figure 4 shows renormalized critical temperatures ($T_c^*/\rho_c^*\tilde{\epsilon}$) as a function of chain length, and Figure 6 shows critical densities for our constant-pressure systems. The imposed pressure was $P^*\sigma^3/\epsilon_{11} = 0$,[32] which essentially corresponds to atmospheric conditions. As for our constant-density simulations, two values of $\tilde{\epsilon}$ were adopted which correspond to systems labeled as P-1 ($\tilde{\epsilon} = 0.01$) and P-2 ($\tilde{\epsilon} = 0.0035$). Note that, for a given $\tilde{\epsilon}$, the polymer mixture can exhibit an upper critical temperature only within a finite range of temperatures, namely, between the glass transition temperature and the vapor−liquid critical temperature. For the $\tilde{\epsilon} = 0.01$ systems, the expected location of T_c for $N = 16$ appears to lie within the glassy region (where the system "freezes" and molecular relaxations become extremely sluggish); conversely, for the $N = 128$ system, T_c lies close to a liquid−vapor transition. For the $\tilde{\epsilon} = 0.0035$ systems, the operative range of temperatures encompasses longer chain lengths, from $N = 64$ up to $N = 380$. The estimated critical temperatures and densities for all constant-pressure systems are also given in Table 1. Note in Figure 6 that the critical density decreases significantly in going from the shortest chain-length systems (leftmost points on the curves) to the longest

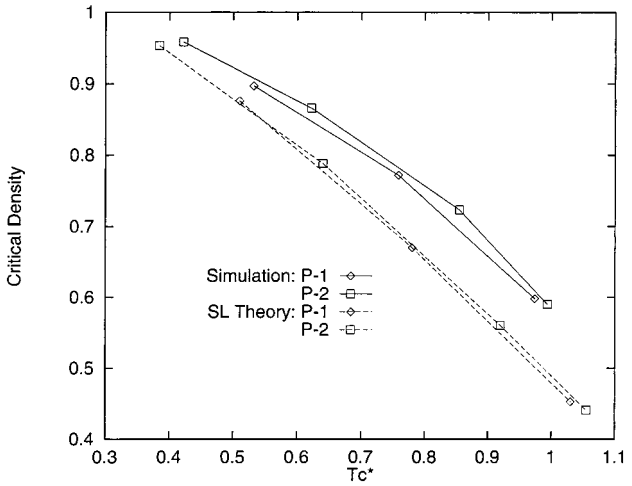

Figure 6. Reduced critical density ρ_c^* as a function of reduced temperature T^* for blends at constant pressure (P-1 and P-2). Simulation data are shown by the full lines and the predictions of Sanchez−Lacombe theory by broken lines.

Table 2. Parameters for the Sanchez−Lacombe Theory of MLJ Systems[a]

parameter	units	value	definition
P_i^*	ϵ/σ^3	5.0	cohesive energy density
v_i^*	σ^3	0.1508	volume of a mer (empty site)
r_i^{o*}	σ^3	$2.5 \times N$	no. of sites occupied by a molecule
Z_{12}		$1.0 - \tilde{\epsilon}$	mixing correction factor

[a] The symbols in the left column are identical to those employed in the original references.[5,6] Variable N is chain length and $\tilde{\epsilon}$ is defined in eq 12.

chain-length polymers (rightmost points). This change in critical density is the result of the thermal expansion of an equimolar liquid polymer blend. For a given chain length, however, the density also changes as the composition changes along the binodal curve. Most of the nonlinear character of the T_c^* vs N relationship can be removed by rescaling T_c^* by a factor of $(\rho^*)^{-1}$ (suggested by eq 4) as shown in Figure 4.

The theory of Sanchez and Lacombe[5,6] was employed to calculate binodal curves and critical temperatures for our constant-pressure MLJ blends. The parameters required by the Sanchez−Lacombe theory are given in Table 2; they were obtained based on select liquid density data for the $N = 64$ and $\tilde{\epsilon} = 0.01$ system and previously reported calculations on MLJ systems.[36] It was assumed that for the range of chain lengths examined here, the molecular size parameter in Sanchez−Lacombe theory (r_i = number of *mers*) is proportional to chain length N (see Table 2). Figure 7 shows a comparison between the predicted and simulated binodal curves. The predicted blend densities are also shown in Figure 6. The theory captures qualitatively the simulated trends of both T_c^* and ρ_c^*; however, it predicts that $T_c^*/\rho_c^* \sim N$ which is not entirely consistent with simulation data (see also next section). The theory also tends to overpredict the changes in critical density with chain length. Both theory and simulation agree, however, in that the $\rho_c^* - T_c^*$ relationship is essentially independent of the chemical mismatch between components over the range of chain lengths examined (e.g., the curves for P-1 and P-2 in Figure 6 are almost indistinguishable).

Constant-pressure phase diagrams for symmetric polymer blends have been reported before by Lifschitz et al.[16] These authors employed a compressible Flory−Huggins theory which reduces to the theory of Sanchez−Lacombe when a purely enthalpic χ parameter is used; results from these (Sanchez−Lacombe type) calculations for atmospheric pressure can be shown to follow the $T_c/\rho_c \sim N$ scaling.[33] Within this formalism, Lifschitz et al. noted that ρ_c becomes unphysically small for N large. Constant pressure calculations for symmetric binary blends of Lennard−Jones chains have been conducted before by Nath et al.[34] and Gromov and de Pablo.[22] Nath et al.[34] implemented a density functional theory that employs correlation functions generated by a PRISM theory. Density changes were introduced by imposing the values obtained from an empirical correlation of experimental data for polyethylene. Nath et al. did observe that T_c of the compressible system was lower than that of the incompressible system, but they did not study the effect of density on the scaling of T_c.

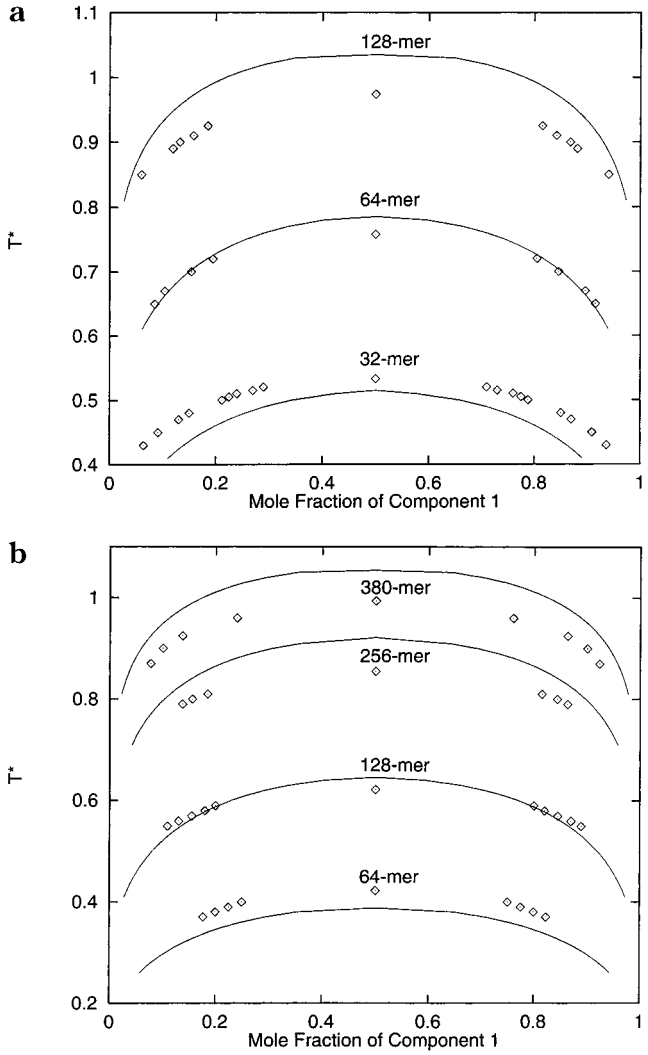

Figure 7. Simulated (symbols) and theoretical (full lines) binodal curves for the MLJ constant-pressure systems. Theoretical curves were calculated by using Sanchez−Lacombe theory with the parameters of Table 2. Part a shows results for system $P - 1$ and part b those for system P-2 (see definitions in the text and in Table 1). Note that the same parameters are used for both systems.

Gromov and de Pablo[22] developed a formalism based on self-consistent PRISM theory and the fluctuation theory of Kirkwood and Buff.[35] This formalism was employed to generate constant-pressure miscibility diagrams for polymer blends; an interaction site was

modeled by a cut-and-shifted Lennard−Jones potential function, which can be described by our MLJ model (eq 11) by setting $\lambda_{ov} = 0$, $\lambda_{cut} = 2.5$, and $\tilde{\epsilon} = 0.1$. For symmetric blends ($N = 16-128$) at $P^* = 1.0$, the theory leads to $T_c^* \sim N^{0.55}$ while expanded-Gibbs ensemble simulation data follow approximately $T_c^* \sim N^{0.47}$ (qualitatively similar results were also reported for blends of square-well chains[24]). On the one hand, these results provide a clear evidence of the importance of density fluctuations and chain length on the scaling of T_c with N. On the other hand, the pressure and temperature ranges covered in these calculations were well above standard experimental conditions; consequently, the critical densities for the long-chain blends were not liquid-like ($\rho_c^* \sim 0.4$ for the 128-mer blend). It is then unclear to what extent these unusual values of pressure and density may contribute to the unexpected scaling of T_c with N. An analysis of Gromov and de Pablo's results shows that $T_c^*/\rho_c^* \sim N^{0.86}$ for PRISM, and $T_c^*/\rho_c^* \sim N^{0.68}$ for simulation; further, their data can also be fitted reasonably well by the relations

$$\text{PRISM:} \quad T_c^*/(\rho_c^*\tilde{\epsilon}) = 13 + 1.7N$$

$$\text{simulation:} \quad T_c^*/(\rho_c^*\tilde{\epsilon}) = 32 + 1.2N$$

which show that PRISM overpredicts the long chain asymptotic value of $T_c^*/(\rho_c^*\tilde{\epsilon}N)$ and underpredicts the short-chain correction constant. These results illustrate the importance of a careful analysis of LLE critical data; different functional forms can be either consistent or inconsistent with the expected long-chain scaling $T_c \sim N$. The next section provides a more detailed discussion of how different scaling forms fit our simulation data.

IV. Analysis of Results

A. Scaling of T_c. Four different models were examined regarding their ability to correlate simulation results:

$$\text{model 1:} \quad \left(\frac{T_c^*}{\rho_c^*\tilde{\epsilon}N}\right) = B + A/N \tag{15}$$

$$\text{model 2:} \quad \left(\frac{T_c^*}{\rho_c^*\tilde{\epsilon}N}\right)^{-1} = B^{-1} + AN \tag{16}$$

$$\text{model 3:} \quad \left(\frac{T_c^*}{\rho_c^*\tilde{\epsilon}N}\right)^{-1} = B^{-1} + A/\sqrt{N} \tag{17}$$

$$\text{model 4:} \quad \left(\frac{T_c^*}{\rho_c^*\tilde{\epsilon}N}\right) = B \times N^{A-1} \tag{18}$$

Models 1, 2, and 3 are based on eqs 7, 6, and 8, respectively; constant A in these models provides a measure of departure from the linear scaling. Constants A and B were calculated by a standard least-squares fit to simulation data. The relative performance of each model can be assessed by comparing the average of the absolute values of the relative deviations between simulated and calculated points; the results are shown in Table 3 for both the constant-density blends and the constant-pressure systems. It is observed that all models are capable of fitting simulation data rather well; it is difficult to discriminate among different two-constant models because only a few data points are available per system.

Table 3. Performance of Different Models for Correlation of Simulated Critical Temperatures

constant	model 1 (eq 15)	model 2 (eq 16)	model 3 (eq 17)	model 4 (eq 18)
system V-0				
A	1.46	7.0×10^{-4}	−0.62	0.96
B	0.84	0.92	0.82	1.04
% error	1.2	2.1	1.2	1.5
system V-1				
A	21.8	4.9×10^{-4}	−2.10	0.88
B	1.20	0.64	1.10	2.53
% error	1.7	1.5	1.4	0.25
system V-2				
A	58.9	6.0×10^{-4}	−3.50	0.82
B	1.23	0.52	1.11	4.08
% error	0.84	2.6	1.0	1.7
system V-3				
A	10.0	6.8×10^{-4}	−1.58	0.90
B	1.07	1.34	0.99	1.93
% error	0.32	4.1	0.8	2.3
system P-1				
A	24.2	2.5×10^{-3}	−2.75	0.73
B	1.11	2.12	0.98	4.75
% error	2.0	2.1	2.1	0.0
system P-2				
A	54.6	8.8×10^{-4}	−3.93	0.74
B	1.13	2.05	1.01	5.62
% error	1.7	5.0	1.8	

Nonetheless, it can be stated that, on average, model 2 leads to higher deviations than the others. Furthermore, since only models 1 and 3 approach $T_c^* \sim N$ for large N, we will concentrate most of our attention on these two models. Constant B in models 1−3 provides an estimate of the expected long chain asymptotic value of $T_c^*/(\rho_c^*\tilde{\epsilon}N)$; the definition of the χ parameter (eq 2) suggests that B should be independent of the strength of chemical mismatch $\tilde{\epsilon}$ between components. This prediction can be tested in the MLJ systems; in fact we find that

$$\text{model 1:} \quad B \approx 1.15 \tag{19}$$

$$\text{model 3:} \quad B \approx 1.03 \tag{20}$$

It is less clear, however, what kind of relationship should hold between A and $\tilde{\epsilon}$. For the MLJ systems we find that

$$\text{model 1:} \quad A \approx 0.56/\tilde{\epsilon}^{0.8} \tag{21}$$

$$\text{model 3:} \quad A \approx -0.38/\tilde{\epsilon}^{0.4} \tag{22}$$

When incompressible and compressible systems with identical $\tilde{\epsilon}$ are compared, parameter A for model 1 is less sensitive to density (and correlates better with $\tilde{\epsilon}$) than that for model 3. Incidentally, model 1 has also been successful at correlating PRISM theoretical predictions (e.g., in ref 12) and lattice simulation data (e.g., in ref 18). Unfortunately, a clear theoretical description of the microscopic contributions to constant A in model 1 is not available. Within the context of the theory of Holyst and Vilgis (model 3), constant A can be regarded as a system-dependent fitting parameter; the term $A/\sqrt{N}$ in eq 17 represents a correction to Flory−Huggins theory that incorporates the effects of concentration fluctuations (fluctuations on a length scale smaller than the polymer radius of gyration $\sim\sqrt{N}$ are unimportant).

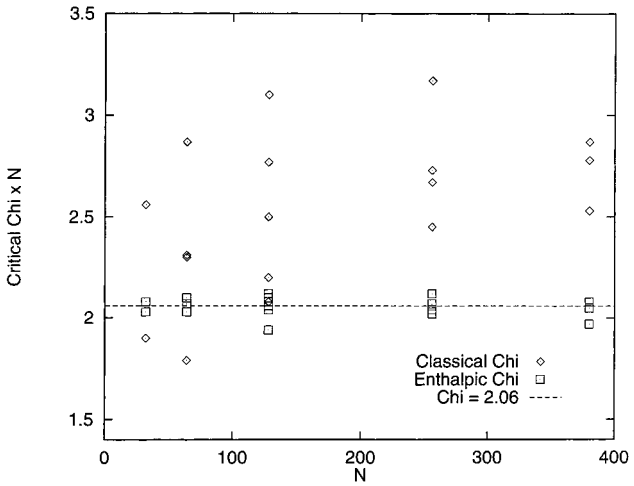

Figure 8. Simulated χ_c parameter as a function of chain length N for all our MLJ systems. The diamonds correspond to a classical mean-field interpretation of χ_c^{MF} (see text) whereby $g_{12}(r) = 1$, and the squares correspond to χ_c^{E} calculated employing simulated values of $g_{12}(r)$.

The net effect of such fluctuations is to promote mixing and thus to lower T_c.

Parameter A in model 4 provides a direct measure of the apparent deviation from $T_c/\rho_c \sim N$. It deviates the least from the expected value $A = 1$ for the repulsive system; the deviation is larger for higher density in the constant-density systems, and it is even larger for the constant-pressure systems. The behavior of the repulsive system is closer to the classical prediction because repulsive chains conform better to the mean-field assumptions (e.g. random mixing and absence of chain correlations). This trend can also be observed in our MLJ systems; the effect of higher temperatures is qualitatively analogous to increasing the chemical mismatch between components (e.g. $T_c \sim \tilde{\epsilon}$). Equations 21 and 22 predict that the correction term (to $T_c \sim N$) will become smaller as $\tilde{\epsilon}$ increases (e.g., the asymptotic regime will be approached for smaller N).

It is less clear why the MLJ constant-pressure systems appear to deviate more from the linear regime than the constant-density blends. Structural information, to be discussed in the next subsection, provides a complementary perspective to this phenomenon. Within the framework of Holyst and Vilgis theory, it could be argued that by allowing density changes, fluctuations of monomer concentration in the system and the associated mean-field corrections are enhanced.

B. Scaling of the χ_c Parameter. The question now arises as to whether the observed deviations from the $T_c \sim N$ scaling are also present in the scaling of χ vs N. The answer depends on the definition adopted for χ. A classical mean-field enthalpic Chi parameter, as defined by eq 2 and to be denoted as χ_c^{MF}, can be calculated from eqs 9 and 10 by introducing a local "random mixing" approximation, e.g. by setting $g_{12}(r) = 1$.[7] The results of such calculations for all our systems are shown in Table 1 and (for MLJ systems only) in Figure 8 (diamonds) as the product of $\chi_c \times N$. Significant deviations are found between simulated $\chi_c^{MF} \times N$ data and the mean-field prediction $\chi_c \times N =$ constant $= 2$. It is clear from Table 1 and Figure 8 that, for any given system, $\chi_c^{MF} \times N$ exhibits an increasing trend with N; in fact, such a systematic trend is the reason a correction term is needed to describe the scaling of T_c vs N over the range of N considered here (as in models 1−4). However, if simulated values of $g_{12}(r)$ (at the critical point) are used in eq 10, the calculated product of $\chi_c^{E} \times N$ is essentially constant with a value close to 2 (see last column in Table 1 and the squares in Figure 8).

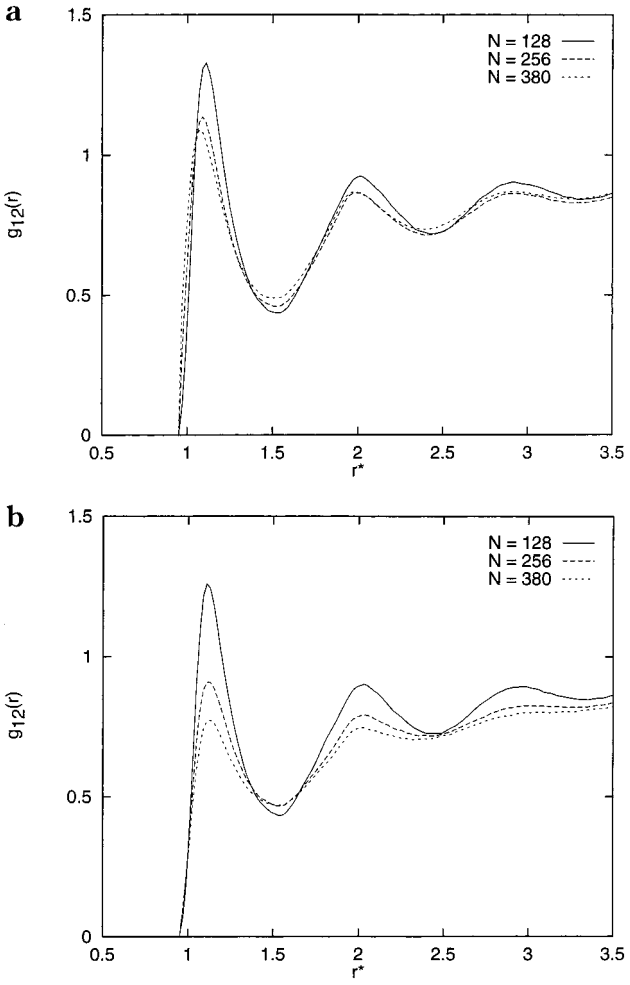

Figure 9. Radial distribution functions for unlike site-site species, $g_{12}(r)$, for (a) system V-2, and (b) system P-2. For clarity, only the region near $r^* = r/\sigma = 1$ is shown; for large r^*, $g_{12}(r) \rightarrow 1$.

The renormalization $\chi_c^{MF} \rightarrow \chi_c^{E}$ is entirely due to the variations of $g_{12}(r)$ (at the critical point) with chain length. Figure 9a shows $g_{12}(r)$ for system V-2; the first peak becomes shorter as N increases. We concentrate mainly on the first solvation layer because it has the greatest impact on thermal interchain interactions. Although variations in $g_{12}(r)$ become less pronounced as N increases, a limiting long-chain "athermal" structure has not been reached yet in our calculations. Figure 9b illustrates the larger renormalization of χ_c^{MF} associated with constant pressure conditions; parts a and b of Figure 9 correspond to critical $g_{12}(r)$ curves for systems V-2 ($\rho^* = 0.9 =$ constant) and P-2 ($P^* =$ constant), respectively, for which the molecular model (and chemical mismatch) are identical. In Figure 9b, the relative change of $g_{12}(r)$ for consecutive chain lengths is more pronounced than that observed in Figure 9a; such a difference is due to the varying density in system P-2 and is consistent with the larger departures from the $T_c \sim N$ scaling observed in constant pressure systems.

Parts a and b of Figure 10 show $g_{11}(r) = g_{22}(r)$ and $g_{12}(r)$ at the critical point for $N = 64$ and 380, respec-

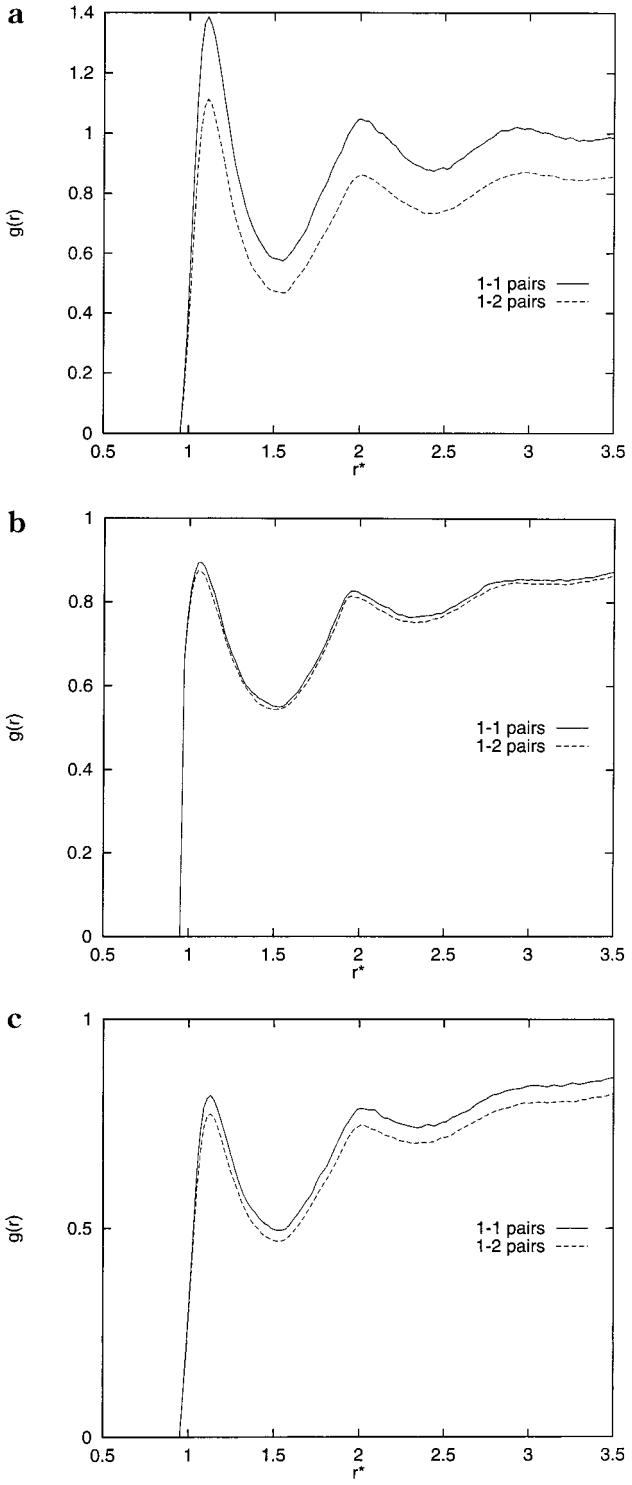

Figure 10. Radial distribution functions for like [$g_{11}(r)$] and unlike [$g_{12}(r)$] species for (a) system V-1 for $N = 64$, (b) system V-1 for $N = 380$, and (c) system P-2 for $N = 380$. For clarity, only the region near $r^* = r/\sigma = 1$ is shown; for large r^*, all radial distribution functions approach unity.

tively, both corresponding to system V-1. Because of the imposed 1-2 chemical mismatch, 1-2 contacts are necessarily less favorable than 1-1 (or 2-2) contacts. The "one-fluid" approximation in which site-site radial distribution functions are assumed to be independent of their type (as in Flory−Huggins theory) is clearly inadequate for $N = 64$, but it becomes fairly accurate for $N = 380$. Figure 10c shows that the difference between $g_{11}(r)$ and $g_{12}(r)$ for $N = 380$, system P-2, is more pronounced than

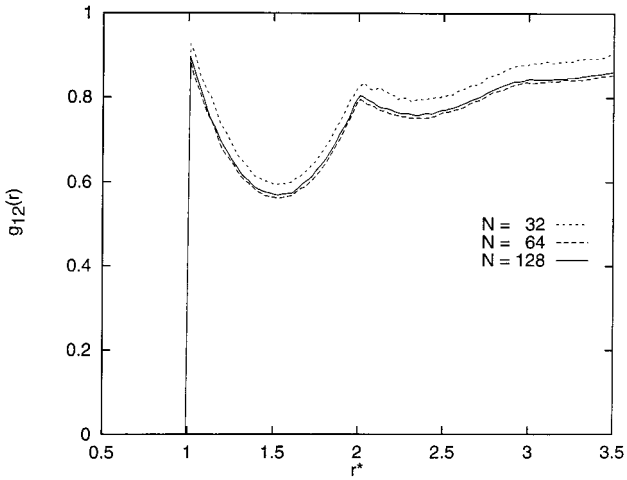

Figure 11. Radial distribution functions for unlike site-site species, $g_{12}(r)$, for the repulsive system (V-0), $r^* = r/\sigma$.

in Figure 10b, even though the chemical mismatch is smaller in system P-2 (N being equal). The reason is that the density and temperature are smaller in Figure 10c. It can then be stated that in the limit of $N \rightarrow \infty$, correlations between unlike species will tend to be screened out only if the (critical) density is sufficiently high. In fact, the relative difference between $g_{11}(r)$ and $g_{12}(r)$ can serve as a guide in experimental work to predict when mean-field scaling predictions will be reliable.

Figure 11 shows $g_{12}(r)$ for the repulsive system V-0. A comparison with Figure 9a for system V-2 confirms the expectation that system V-0 approaches a limiting fluid structure for shorter chain lengths than system V-2. A peculiarity of system V-0 is, however, that the finite value of $g_{12}(r)$ at contact ($r = \sigma$) does not monotonically decrease as N increases. Specifically, at short distances, $g_{12}(r)$ for $N = 128$ is slightly larger than for $N = 64$. The reason is that the local fluid structure is affected by two competing effects. On the one hand, a longer N leads to a stronger correlation hole effect which tends to reduce $g_{12}(r)$. On the other hand, a longer N implies a higher T_c and weaker relative mismatch; thus, $g_{12}(r) \rightarrow g_{11}(r)$. For our particular model, V-0, it appears that for $N > 64$ the second effect becomes more important that the first.

To the best of our knowledge, this is the first simulation study that provides a direct evidence for the validity of $\chi_c^E \times N = \text{constant} = 2$ for symmetric polymer blends; previous simulation studies indicate or imply a significant renormalization of the numerical constant.[18,21] Although eq 10 is only approximate,[38] the fact that all systems obey eq 3 regardless of different chemical mismatch, chain length, density, molecular force field and for either constant density or constant pressure conditions, provides compelling evidence in favor of such scaling law, even for relatively short polymers. The scatter in the $\chi_c^E \times N$ data shown in Figure 8 can be entirely attributed to simulation errors associated with the estimation of the critical point. That the simulated average value of $\chi_c^E \times N$ is 2.06 and not 2.00 (only 3% off) can be rationalized by the effect of systematic deviations in the calculation of T_c and χ_c^E due to finite size effects and the approximations associated with the definition of χ^E.

It is finally pointed out that our results for χ^E also help explain why experimental data are consistent with

the mean-field scaling $\chi_c \sim N$;[23] as it is usually the case, χ_c is extracted from small-angle neutron scattering data which inherently contain information about the local fluid structure. Consequently, experimentally measured χ^{SANS} parameters effectively capture the correlation hole effect and other factors that affect $g_{12}(r)$; the formal connection between the estimation of χ from experiment and simulation has been described elsewhere.[18,21,26]

V. Conclusions

Semigrand ensemble Monte Carlo simulations and histogram reweighting techniques have been employed to determine the phase diagram and critical temperature of binary, symmetric polymer blends. Two types of polymer mixtures were simulated by changing the relative strength of like-species attractive interactions (e.g. attractive and repulsive systems). The scaling of the critical temperature and χ parameter with chain length has been determined for both constant-density and constant-pressure systems. For the range of chain lengths examined in this work (from $N = 32$ up to 380 sites), small but significant departures were observed from Flory's long-chain scaling law $T_c \sim N$; good agreement was found, however, with the prediction of $\chi_c \sim 2/N$.

A polymer site in our fully flexible MLJ chains corresponds to N_r consecutive repeat units in a real polymer, where N_r should be sufficiently large to represent a Kuhn segment (e.g., the persistence length). For typical synthetic polymers, $N_r \sim 10$, which translates into a molecular weight of 100 to 200 per MLJ site for simple polyolefins.[37] A range from $N = 32$ to 380 then corresponds to polymers with molecular weights in the range 5×10^3 to 5×10^4. Accordingly, our simulation results show that noticeable deviations from the simple $T_c \sim N$ scaling could occur for polymers with molecular weights as high as $O(10^5)$. This conclusion is significant, as polymers with such molecular weights are not uncommon in practical applications. The deviations decay as N is increased; for example, they go from ~50% to ~5% (of T_c) as the polymer molecular weight increases from $N = 64$ to $N = 380$ in our $\rho^* = 0.825$ blends. As suggested by our results shown in Figures 5 and 7, the practice of fitting experimental data for just one polymer molecular weight to a Flory−Huggins type theory can lead to incorrect predictions of miscibility for polymers of different molecular weights. It is highly recommended that the critical temperature be obtained for at least two polymer chain lengths; this will provide a minimum data set for a two-constant empirical correlation for T_c vs N.

Our results and conclusions are consistent with the predictions of the theory of Holyst and Vilgis;[9] unfortunately, the range of chain lengths examined in this work is not sufficiently wide to discriminate between different models of T_c vs N. In particular, it was found that $T_c/\tilde{\epsilon}$ scales approximately as either $\rho_c(A + BN)$ or $\rho_c N/(B^{-1} + A/\sqrt{N})$; for the MLJ systems, the former model leads to parameters A and B that are less sensitive to the system's density. The approach to the expected mean-field linear regime where $T_c \sim N$ is favored by higher temperatures, a large chemical mismatch between the components or predominantly repulsive interaction forces, and constant density conditions (as opposed to constant pressure conditions).

While deviations from the mean-field prediction $T_c \sim N$ can be significant for the range of chain lengths spanned in our simulations, the classical result $\chi_c \sim N$ has been shown to be accurate, provided that a definition for χ is used in which variation of the local fluid correlations is properly accounted for. We find that χ_c^E as defined by eqs 9 and 10 conforms to the mean-field relationship $\chi_c^E \sim 2/N$, regardless of the system's density, chemical mismatch or molecular model adopted. The analysis of radial distribution functions at the critical point clearly shows the correlation between fluid structure and the observed trends for the scaling and deviations of T_c with chain length.

Acknowledgment. The authors are grateful to one of the reviewers of this manuscript for pointing out ref 26 and suggesting additional calculations for the enthalpic χ parameter. Financial support from the National Science Foundation (CTS-9629135) is gratefully acknowledged. J.J.d.P. is also grateful to the Camille and Henry Dreyfus Foundation for a Teacher−Scholar Award.

References and Notes

(1) Flory, P. J. *Principles of Polymer Chemistry*; Cornell University Press: New York, 1953.
(2) Singh, C.; Schweizer, K. S. *J. Chem. Phys.* **1995**, *103*, 5814. Weinhold, J. D.; Kumar, S. K.; Singh, C.; Schweizer, K. S. *J. Chem. Phys.* **1995**, *103*, 9460.
(3) Kumar, K. S.; Weinhold, J. D. *Phys. Rev. Lett.* **1996**, *77*, 1512.
(4) Escobedo, F. A.; de Pablo, J. J. *J. Chem. Phys.* **1997**, *106*, 9858.
(5) Sanchez, I. C.; Lacombe, R. H. *J. Phys. Chem.* **1976**, *80*, 2353. Lacombe, R. H.; Sanchez, I. C. *J. Phys. Chem.* **1976**, *80*, 2568.
(6) Sanchez, I. C.; Lacombe, R. H. *Macromolecules* **1978**, *11*, 1145.
(7) Schweizer, K. S.; Curro, J. G. *J. Chem. Phys.* **1989**, *91*, 5059; *Adv. Chem. Phys.* **1997**, *98*, Chapter 1.
(8) deGennes, P. G. *Scaling Concepts in Polymer Physics*; Cornell University, Ithaca, NY, 1979.
(9) Holyst, R.; Vilgis, T. A. *J. Chem. Phys.* **1993**, *99*, 4835.
(10) A treatment similar to that given in ref 9 has been presented by: Garas, G. E.; Kosmas, M. K. *J. Chem. Phys.* **1995**, *103*, 10790.
(11) Bates, F. S. *Science* **1991**, *251*, 898.
(12) Yethiraj, A.; Schweizer, K. S. *J. Chem. Phys.* **1993**, *98*, 9080.
(13) Schweizer, K. S.; Yethiraj, A. *J. Chem. Phys.* **1993**, *98*, 9053.
(14) Dudowicz, J.; Freed, K. F. *Macromolecules* **1991**, *24*, 5112; *J. Chem. Phys.* **1992**, *96*, 1644.
(15) Dudowicz, J.; Lifschitz, M.; Freed, K.; Douglas, J. F. *J. Chem. Phys.* **1993**, *99*, 4804.
(16) Lifschitz, M.; Dudowicz, J.; Freed, K. *J. Chem. Phys.* **1994**, *100*, 3957.
(17) Sariban, A.; Binder, K. *J. Chem. Phys.* **1987**, *86*, 5859. Sariban, A.; Binder, K. *Macromolecules* **1988**, *21*, 711.
(18) Deutsch, H.-P.; Binder, K. *Macromolecules* **1992**, *25*, 6214.
(19) Deutsch, H.-P. *J. Stat. Phys.* **1992**, *67*, 1039.
(20) Müller, M.; Wilding, N. B. *Phys. Rev. E* **1995**, *51*, 2079.
(21) Grest, G. S.; Lacasse, M.-D.; Kremer, K.; Gupta, A. M. *J. Chem. Phys.* **1996**, *105*, 10583.
(22) Gromov, D.; de Pablo, J. J. *J. Chem. Phys.* **1998**, *109*, 10042.
(23) Gehlsen, M. D.; Rosedale, J. H.; Bates, F. S.; Wignall, G. D.; Hansen, L.; Almdal, K. *Phys. Rev. Lett.* **1992**, *68*, 2452.
(24) Escobedo, F. A. Ph.D. Thesis, University of Wisconsin−Madison, 1997.
(25) Yethiraj, A.; Dickman, R. *J. Chem. Phys* **1992**, *97*, 4468.
(26) Müller, M.; Binder, K. *Macromolecules* **1995**, *28*, 1825.
(27) Escobedo, F. A.; de Pablo, J. J. *J. Chem. Phys.* **1996**, *104*, 4788.
(28) Ferrenberg, A. M.; Swendsen, R. H. *Phys. Rev. Lett.* **1989**, *63*, 1195.
(29) Wilding, N. B. *Phys. Rev. E* **1995**, *52*, 602.
(30) Ferrenberg, A. M.; Swendsen, R. H. *Phys. Rev. Lett.* **1988**, *61*, 2635.
(31) Allen, M. P.; Tildesley D. J. *Computer Simulation of Liquids*, Clarendon Press: Oxford, England, 1987.

(32) A zero pressure is actually inconsistent with a stable liquid phase. However, the properties of the system do not change significantly if a finite but small pressure (like the atmospheric pressure) is employed.

(33) It is expected that the lattice-cluster theory[14] and the Sanchez−Lacombe theory will lead to similar scaling forms (for the systems studied in this work).

(34) Nath, S. K.; McCoy, J. D.; Curro, J. G.; Saunders: R. S. *J. Polym. Sci., Part B* **1995**, *33*, 2307.

(35) Curro, J. G.; Schweizer, K. S. *Macromolecules* **1991**, *24*, 6736.

(36) Escobedo, F. A.; de Pablo, J. J. *J. Chem. Phys.* **1999**, *110*, 1290.

(37) Gromov, D. G.; de Pablo, J. J.; Luna-Barcenas, G.; Sanchez, I. C.; Johnston, K. P. *J. Chem. Phys.* **1998**, *108*, 4647.

(38) A more accurate expression of an enthalpic, off-lattice χ parameter has been given by Tillman et al.[39] (eq 3.5). The final conclusions of an analysis based on such an equation would be, however, analogous to those based on eq 9.

(39) Tillman, P.; Rottach, D. R.; McCoy, J. D.; Plimpton, S. J.; Curro, J. G. *J. Chem. Phys.* **1998**, *109*, 806.

MA9812276